01

Star imaging under the influence of angular anisoplanatism in turbulent atmosphere

© V.A. Bogachev,[1] A.V. Nemtseva,[1,2] F.A. Starikov[1,3]

[1] Russian Federal Nuclear Center, All-Russian Research Institute of Experimental Physics,
Sarov, Nizhny Novgorod region, Russia
[2] Faculty of Physics of Lomonosov Moscow State University, Branch of Lomonosov Moscow State University in Sarov
Sarov, Nizhny Novgorod region, Russia
[3] Sarov Physical and Technical Institute branch of National Research Nuclear University „Moscow Engineering Physics Institute“,
Sarov, Nizhny Novgorod region, Russia
e-mail: bogachev.v@mail.ru

Received February 28, 2024
Revised April 3, 2024
Accepted April 12, 2024

Three-dimensional numerical simulation of the propagation of radiation from a natural star through a turbulent atmosphere to a telescope located on the Earth as well as its imaging with the help of adaptive optics and a reference source technique, has been carried out. The verification of the calculation model has been performed. The accuracy of determining the angular coordinate of the star using radiation of another natural star located outside the isoplanar region at different outer scales of turbulence has been investigated and compared with approximate analytical data.

Keywords: numerical simulation, turbulent atmosphere, outer scale of turbulence, angular anisoplanatism, adaptive phase correction.

DOI: 10.61011/TP.2024.06.58818.59-24

Introduction

This paper reviews issues of interest for astronomy and laser location of remote objects. The objective to observe space objects located at a very large (stars) and at a finite distance from a telescope is relevant for astronomy. The objective of laser location of a space object moving in the near-Earth orbit is of special interest in connection with the problems of the space laser communication [1], and also with the pollution of the near-Earth space by space debris, the considerable part of which is not catalogued [2]. In both cases the quality of the space object image is substantially affected by the atmospheric turbulence.

In state-of-the-art ground astronomic observatories, adaptive optical systems (AOS) are used to compensate adverse impact of the atmospheric turbulence [3–6]. The essence of the AOS operation consists in measurement of optical distortions on the way of light travelling in the atmosphere to the telescope and introduction of the required phase distortions that compensate turbulence impact using an adaptive mirror. For this purpose both the emission from the observed object itself and emission from an artificial source „ignited“ in its direction — laser guide star (LGS) [7] can be used. The last case is relevant, if the object has low brightness or has no astronomical sources bright enough nearby. Besides, the object of interest and LGS must be located within the isoplanar region, i. e. the angular distance between them must be rather small, so that the light from the object and LGS passes through the same optical inhomogeneities. In real AOSs the efficiency of using the Rayleigh LGS is limited the height of 10−20 km above the Earth's surface owing to decrease of the Rayleigh scattering efficiency along with height increase. LGS formation in the sodium layer at height of 90−100 km is more preferable, since in this case optical inhomogeneities of the entire meaningful atmosphere column are compensated.

Using the LGS approach is coupled with the problem of finding the global tilt of the wavefront [8]. A laser beam creating LGS and radiation from LGS, captured by the telescope, pass through the same atmospheric optical „wedge“, which makes it impossible to determine the value of the reference emission wavefront tilt. Various approaches to solution of this problem are studied [9–12], where numerical simulations plays a critical role [13,14]. Comparison of the results of analytical estimates and numerical modeling of light propagation through the turbulent atmosphere makes it possible to verify the numerical model and to understand in more detail the impact of various effects at quality of an astronomic object image formed using adaptive optics.

Currently, when the laser space communication systems are developed [1], one of the key problems is the problem of precise positioning of the transmitted signal on a remote receiver [15–17]. Experimental data on mutual correlation of wavefront tilts from double stars turn out to be quite useful [18,19]. For example, in paper [19] such data is provided for the three pairs of stars at a different angular distance between them, and also for one double star at different

values of the angle of elevation. Naturally, the experimental data was obtained under certain conditions of optical weather. Numerical estimates present higher flexibility in variation of both parameters of the outgoing laser radiation and turbulent path, along which it propagates [20,21]. However, when performing numerical calculations, it is necessary to take into account the finiteness of the outer scale of turbulence as a parameter determining large-scale optical aberrations.

The objective of this paper is computational study of the possibility to generate a diffraction image of a natural star and precision of its angular coordinate determination using adaptive optics and joint use of reference radiation of two types — from LGS, ignited in its direction, and the second star at the angular distance substantially exceeding the classic angle of isoplanatism. Results obtained in 3D calculations at different external scale of turbulence are compared to the analytic assessments available in the literature.

1. Problem formulation

The scheme of the problem is shown in Fig. 1. Two natural stars are observed via a telescope located on the Earth. Angular distance between them is $\alpha = 10\,\text{arcsec} = 48.5\,\mu\text{rad}$ — by 5 arcsec to the left and right (along the axis x) from the vertical direction z. For an observer on the Earth the stars are actually the point sources of light. Since they are located at a great distance, the curvature of the wavefront of their radiation that reached the Earth is a negligibly low value. We believe that radiation

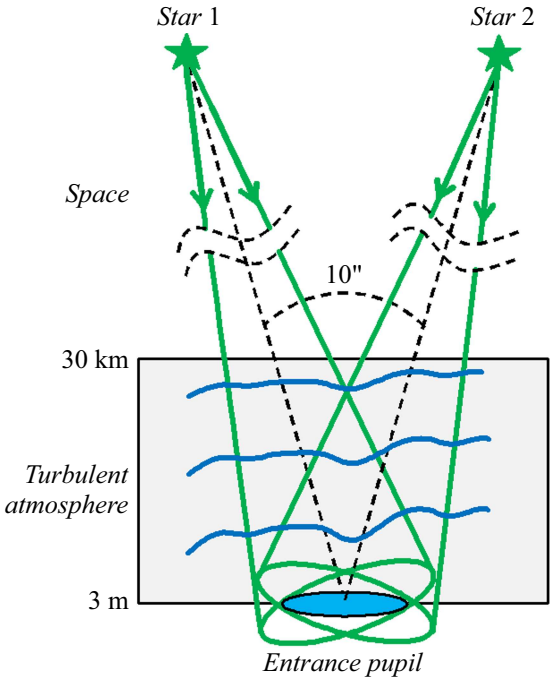

Figure 1. Scheme of problem of angular anisoplanatism investigation.

from each star at the upper boundary of atmosphere has a flat wavefront, which, passing via atmosphere, acquires phase distortions. Light from stars observaed by the telescope with a round entrance pupil either directly, or after passage via AOS, is focused by a lens to obtain a star image.

In calculations, the altitude model of structural characteristic of the air refraction index is used $C_n^2(h)$ [22]. In the surface layer $C_n^2 = 2 \cdot 10^{-15}\,\text{cm}^{-2/3}$, which is compliant with the night observations on the flat terrain. It is known that the main spatial parameters characterizing the influence of atmosphere turbulence on light radiation are Fried parameter r_0, angle of isoplanatism θ_0 and isokinetic angle θ_T. Parameter θ_0 characterizes the region of isoplanatism tacking into account of all optical aberrations, and parameter θ_T — taking into account only tilts of the wavefront along the x- and y-axes.

In case of Kolmogorov spectrum of air refraction index fluctuations, parameters r_0, θ_0 and θ_T are defined as [4]:

$$r_0 = \left(0.423k^2(\sec\xi)\int\limits_{h_0}^{h_{\max}} C_n^2(\xi)d\xi\right)^{-3/5}, \qquad (1)$$

$$\theta_0 = \left(2.914k^2(\sec\xi)^{8/3}\int\limits_{h_0}^{h_{\max}} C_n^2(\xi)\xi^{5/3}d\xi\right)^{-3/5}, \qquad (2)$$

$$\theta_T = \left(0.668k^2D^{-1/3}(\sec\xi)^3\int\limits_{h_0}^{h_{\max}} C_n^2(\xi)\xi^2 d\xi\right)^{-1/2}, \qquad (3)$$

where λ and $k = 2\pi/\lambda$ — wavelength and wave number of radiation, ξ — zenith angle, D — diameter of receiving aperture of the telescope, h_0 — height of receiving aperture of the telescope above Earth's surface, $h_{\max}$ — height of the upper boundary of atmosphere. For the parameters set in the calculations: $\lambda = 0.55\,\mu\text{m}$, $\xi = 0^\circ$, $D = 1\,\text{m}$, $h_0 = 3\,\text{m}$, $h_{\max} = 30\,\text{km}$ we obtain that $r_0 = 5.9\,\text{cm}$, $\theta_0 = 0.6\,\text{arcsec}$, $\theta_T = 2.13\,\text{arcsec}$. It is important to note that $\theta_T < \alpha$ and $\theta_0 \ll \alpha$. Analytic formulae for r_0, θ_0, θ_T (1)–(3) are the limit ones (bottom estimate), since in the Kolmogorov model of turbulence the inner scale of distortions is $l_0 = 0$, and the outer scale is $L_0 = \infty$. In reality parameters l_0, L_0 take on finite values.

2. Computational model

The light radiation propagation in the turbulent atmosphere was calculated within integration of parabolic equation for the complex amplitude of the radiation field [23]:

$$2ik\frac{\partial E}{\partial z} + \frac{\partial^2 E}{\partial x^2} + \frac{\partial^2 E}{\partial y^2} + k^2\varepsilon E = 0, \qquad (4)$$

where $E(x, y, z)$ — complex amplitude of the electric field strength, $\varepsilon(x, y, z)$ — function describing fluctuations of the dielectric permittivity of the medium. Equation (4)

was solved numerically using the finite-difference scheme of Ladagin [24], having zero amplitude error and phase error of the fourth order with integration of a diffraction operator. A continuous randomly inhomogeneous medium was replaced with an equivalent chain of phase screens. The von Karman model of the spatial spectrum of refractive index fluctuations was used in the calculations [25]:

$$\Phi_n(\kappa_\perp, \kappa_z) = 0.033 C_n^2 (\kappa_\perp^2 + \kappa_z^2 + \kappa_0^2)^{-11/6}, \qquad (5)$$

where $\kappa^2 = \kappa_\perp^2 + \kappa_z^2 = \kappa_x^2 + \kappa_y^2 + \kappa_z^2$, κ — spatial frequency, $\kappa_0 = 2\pi/L_0$ — lowest spatial frequency, L_0 — outer scale of turbulence. The highest spatial frequency $\kappa_m = 2\pi/l_0$ corresponds to the inner scale of turbulence l_0. Contribution to „energy" of turbulence from the lowest scales is negligible, therefore for spectrum (5) $l_0 = 0$. In the inertial interval $2\pi L_0^{-1} \le \kappa \le 2\pi l_0^{-1}$ the von Karman spectrum corresponds to the theory of Kolmogorov–Obukhov [26,27].

For the von Karman spectrum the following analytical formula is known for calculation of the correlation function of phase on a thin phase screen [28]:

$$B_\varphi(r) = \sigma_\varphi^2 \frac{2^{1/6}}{\Gamma(5/6)} (\kappa_0 r)^{5/6} \mathrm{K}_{5/6}(\kappa_0 r), \qquad (6)$$

$$\sigma_\varphi^2 = 2.4\pi^2 k^2 \kappa_0^{-5/3} (0.033 C_n^2 \Delta z), \qquad (7)$$

where r — distance between two screen points, $\Gamma(-)$ — gamma function, $\mathrm{K}(-)$ — Macdonald function, σ_φ^2 — dispersion of phase fluctuations on the screen, Δz — thickness of turbulent layer replaced with a phase screen, $C_n^2 = \mathrm{const}$. For the vertical path modeled by a combination of phase screens, we use in the formula (7) $\int_{h_0}^{h_{\max}} C_n^2(\xi) d\xi$ instead of $C_n^2 \Delta z$. The structural function of the phase was calculated using equation

$$D_\varphi(r) = 2\big(B_\varphi(0) - B_\varphi(r)\big). \qquad (8)$$

In the computational model the turbulent path was replaced with a chain of M phase screens, δ-correlated along z direction [29,30]. The structural function of the phase for the chain of screens was calculated as a sum of structural functions of individual screens i. e.

$$D_\varphi^{\mathrm{num}}(r) = \sum_{i=1}^{M} D_i^{\mathrm{num}}(r).$$

Since the used model complies with the conditions of locally homogeneous and isotropic turbulence, calculation of $D_i^{\mathrm{num}}(r)$ on a grid was carried out along one identified direction on ith phase screen using a correlation function calculated in the grid nodes:

$$B_i^{\mathrm{num}}(l) = \frac{1}{(N-l)} \sum_{m=1}^{N-l} \tilde{\varphi}_i(m, N/2) \tilde{\varphi}_i^*(m+l, N/2), \qquad (9)$$

where $\tilde{\varphi}_i(m, n)$ — random implementation of the complex phase field [28], N — even number of computational grid nodes, $l = 0, \ldots, N-1$.

In the spectral method [29] the random phase field is formed using filtration of the Gaussian pseudorandom field, and the transfer function of the filter depends on the spatial spectrum of phase fluctuations. This method makes it possible to form phase screens with $L_0 \le A/2$, where A — transverse size of the countable domain. In the calculations $A = 5.12$ m, which makes it possible to correctly model phase distortions with L_0 up to 2.56 m. Minimum size of distortions $l_0 \approx 2s$ [29] is equal to 5 mm, where s — computational grid pitch.

To model large-scale distortions at $L_0 > A/2$ and maintain the size of the countable domain, additionally the subharmonics method was used [28,31]. The substance of this method consists in subsequent addition of spatial harmonics with the period exceeding the size of the countable domain into the spectrum of phase fluctuations. This procedure is carried out by serial (iteration) densification of the computational grid nodes in the spectral plane $(\Delta\kappa_x, \Delta\kappa_y)$ in the vicinity of zero harmonic. In accordance with [31] on each jth iteration, additional 32 harmonics are added to the phase spectrum with pitch $\Delta\kappa_x/3^j$ and $\Delta\kappa_y/3^j$, which are calculated in the rectangular area of the spectral space limited by points with coordinates $(\pm\Delta\kappa_x/3^{j-1}, \pm\Delta\kappa_y/3^{j-1})$, $j = 1, 2, \ldots, J$. Therefore, accuracy of reproduction of the low-frequency part of the phase spectrum increases by increasing the number of iterations J. The resulting phase field is found in the form of the sum of its high frequency part produced by spectral method, and low frequency part generated with subharmonics. The structural function of the phase on jth iteration is a sum of structural functions of the high frequency part of the phase and its low frequency part to the jth iteration inclusive.

Fig. 2 presents structural functions of the phase calculated at different values L_0. If L_0 increases, the absolute values of function $D_\varphi(r)$ increase. As follows from Fig. 2, *a*, the structural function of the phase on the grid lattice is indeed close to the analytical one at $L_0 = A/2 = 2.56$ m. When only the spectral method is used, the error of the modeled structural function of the phase increases with increase of L_0 — on the receiving aperture it reaches 2, 37, 44 and 56% at L_0, equal to 2.56, 20, 40 and 1000 m accordingly. With increase of the number of subharmonic levels the calculated structural function practically matches the analytical one, which confirms adequate modeling of the turbulent field of the refraction index fluctuations. It should also be noted that the need for accounting of finiteness L_0 increases with the increase of the telescope receiving aperture.

Therefore, the phase screens formed with the help of a combination of the spectral method with the method of subharmonics make it possible to build a numerical turbulence model taking into account the effect of large scale spatial inhomogeneities exceeding the size of the countable domain at the nature of the beam propagation

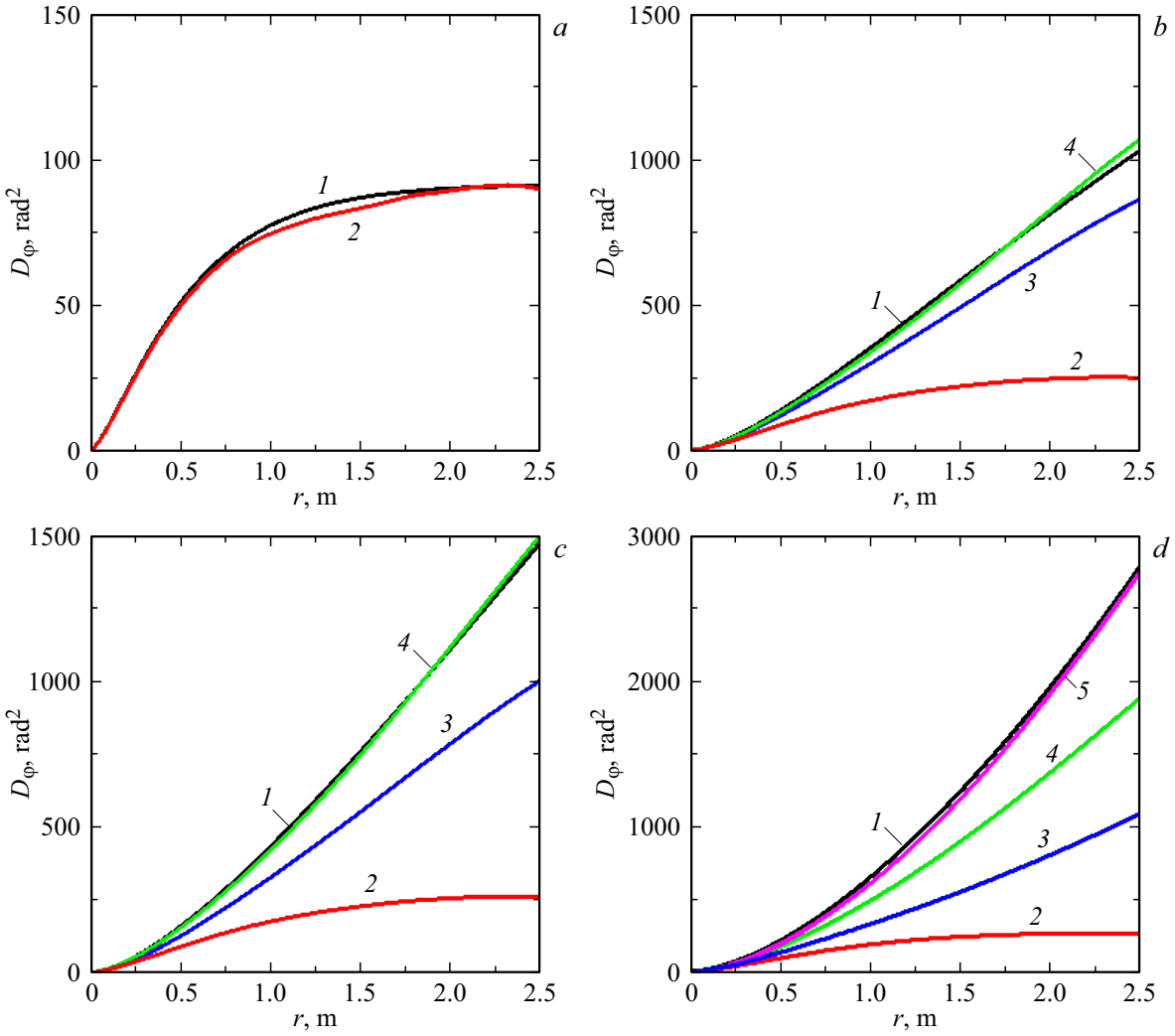

Figure 2. Analytical (*1*) and calculated structural functions of the phase obtained by the spectral method (*2*) and with additional use of the subharmonic method at $J = 1$ (*3*), 2 (*4*), 4 (*5*) for L_0, equal to 2.56 (*a*), 20 (*b*), 40 (*c*), 1000 m (*d*).

in the atmosphere. Below this model was used to present a vertical turbulent path with a chain of phase screens that were generated by the above method.

3. Results of numerical simulation

Fig. 3 presents calculated distributions of radiation intensity $I_{NF}(x/D, y/D)$ from stars 1 and 2 in the near field on the receiving round aperture in one realization of turbulent atmosphere at $L_0 = 20$ m. Fig 4 shows images of stars, i. e. distributions of their radiation intensity in the far field $I_{FF}(\theta_x, \theta_y)$, displaced by angle $+5$ arcsec and -5 arcsec from the axis in direction x. Values of intensity I_{NF} and I_{FF} are normalized by the corresponding maximum values I_{NF}^{vac} and I_{FF}^{vac} in case of beam passage in vacuum. Distributions $I_{NF}(x/D, y/D)$ and $I_{FF}(\theta_x, \theta_y)$ have a clearly expressed heterogeneous structure, besides, it is different for two paths. This already indicates anisoplanatism of paths, at least by high-order aberrations.

The image quality in the far field specifies effect of turbulence on radiation, the spot size substantially exceeds the diffraction size $\theta_{\text{dif}} = 0.28$ arcsec, where $\theta_{\text{dif}} = 2.44\lambda/D$. In Kolmogorov turbulence model the angular full-width at half maximum of the star image θ_{FWHM} under long-term exposure is related to Fried radius as $\theta_{FWHM} = 0.98\lambda/r_0$ [32]. Using this formula, let us assess the radius of atmosphere coherence ρ_0 (analog of parameter r_0 at finite L_0) in case of Karman model. Long-term exposure was simulated by averaging of 100 star images corresponding to various realizations of the turbulent paths. In the calculations it was obtained that $\rho_0 = 7.4$ cm at $L_0 = 20$ m, i. e. finiteness of the external turbulence scale increases the coherence radius (remember that $\rho_0 = r_0 = 5.9$ cm at $L_0 = \infty$). Dependence $\rho_0(L_0)$ will be presented below.

Fig. 5 shows distribution of radiation phase in near field from each star and their difference in this realization of

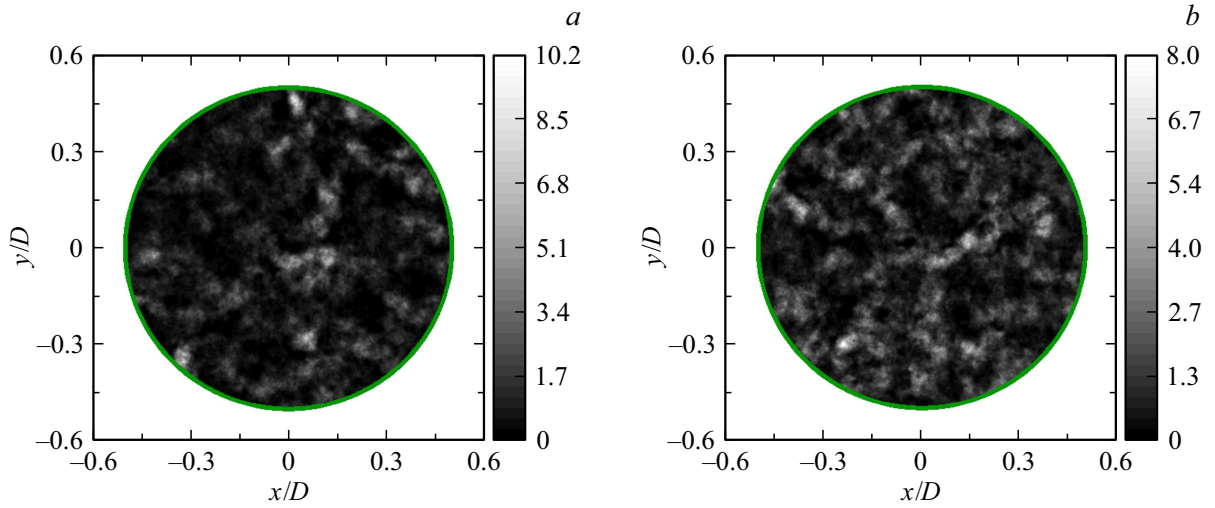

Figure 3. Instantaneous distribution of normalized radiation intensity of star 1 (*a*) and 2 (*b*) in the near field.

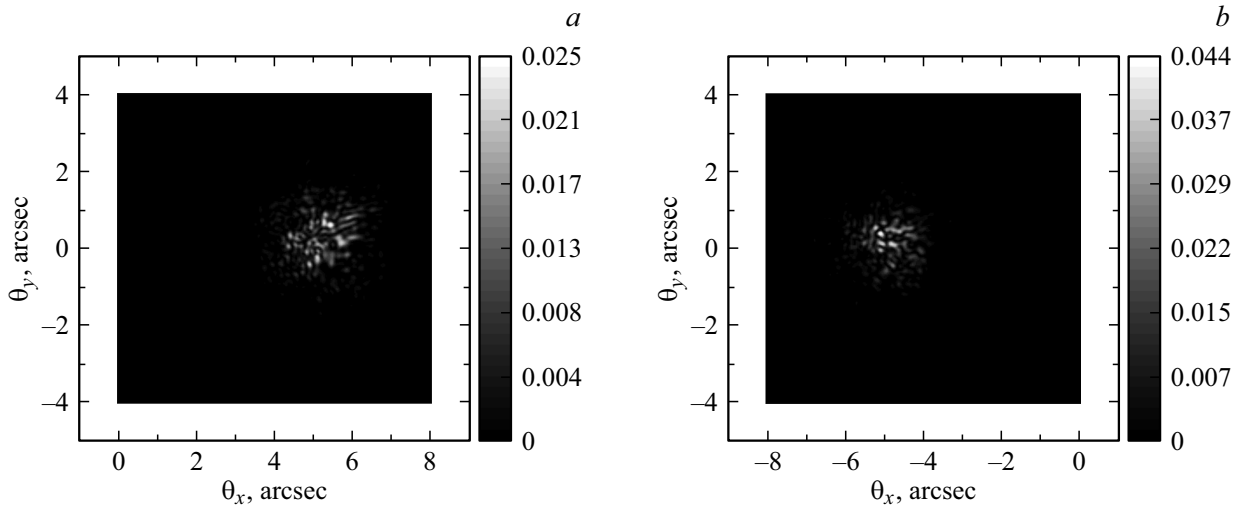

Figure 4. Instantaneous distribution of normalized radiation intensity of star 1 (*a*) and 2 (*b*) in the far field.

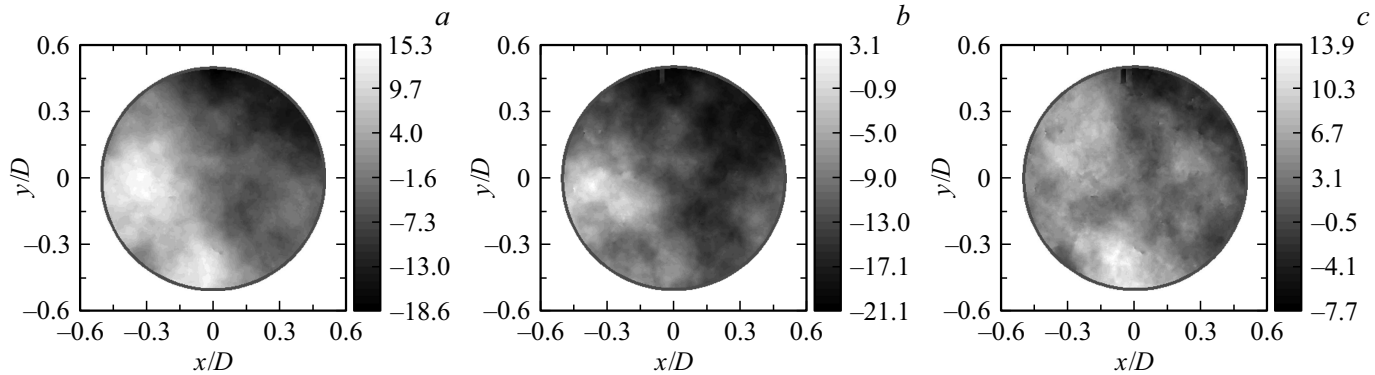

Figure 5. Distribution of radiation phase (in rad) from star 1 (*a*) and 2 (*b*) and their difference (*c*).

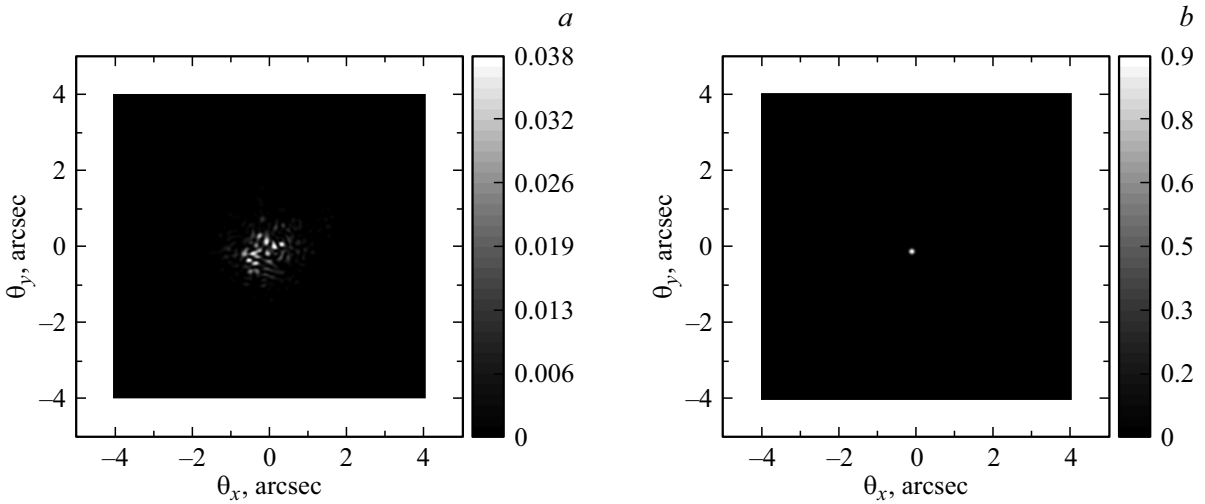

Figure 6. Distribution of normalized intensity of star 2 at phase correction by wavefront from star 1 (a), at phase correction by its higher aberrations and tilts of the wavefront from star 1 (b).

atmosphere (tilts of optical axes from the vertical line by ± 5 arcsec are not taken into account). Unwrapping of the phase cleared its surges at 2π [33]. With the substantially heterogeneous pattern of intensity in Fig. 3 the phase distribution is regular (in some areas of the phase surface small artifacts have remained, which do not complicate the pattern perception as a whole).

For the phase surface of radiation of stars 1 and 2 the parameter PV (peak-to-valley), i. e. the maximum phase difference on the aperture is equal to $PV = 33.9$ and 24.2 rad accordingly, and for phase difference — $PV = 21.6$ rad. Even though phase surfaces of radiation from both stars in general remind each other, their difference gives a comparable value PV. This already indicates a certain degree of isoplanatism by low-order aberrations and its absence in the entire totality of aberrations, which by impact at image quality is similar to the case of incomplete phase conjugation [34,35].

Let us now imagine that star 2, the clear image of which we must obtain, has such small star value, that it is not possible to measure the wavefront of its radiation — a problem of weak signal so well known in astronomy (small size of space debris or low stellar brightness). Then let us build the image of star 2 in the far field at phase correction of its radiation, adding with the help of the imaginary adaptive mirror a phase screen conjugated with the phase of radiation from bright star 1. In this case after passage of the adaptive mirror the radiation of star 2 will acquire a differential phase front (Fig. 5, c). Image of star 2 is shown in Fig. 6, a. Its complete angular size by energy level 95% after averaging is equal to 6 arcsec, which approximately coincides with the case without correction (Fig. 4, b). This is the manifestation of anisoplanatism by all aberrations, i. e. use of star 1 as a reference source for correction of phase distortions from star 2 is absolutely inefficient.

Since it is not possible to restore the wavefront of radiation of star 2 due to its low brightness, a sodium LGS may be „ignited“ in its direction. But LGS is formed with the help of a laser located on the Earth, therefore, a problem of uncertainty of LGS angular coordinate arises (i. e. global tilt of wavefront) [9–11]. Therefore, to control the adaptive mirror, we use high-order (except for wavefront tilt) aberrations from LGS radiation, and tilt — from radiation of the bright neighboring star 1, remembering a certain degree of isoplanatism of paths by lower aberrations. Fig 6, b shows image of star 2 at phase correction by high-order aberrations of LGS (in neglection of cone effect [4]) and tilts of the wavefront from star 1. Here the image is ideal, but it is deviated from the axis by the difference of two tilts. Then let us find the error in detection of the angular coordinate of star 2 by this method.

Tilt of the star wavefront may be identified by two methods: by center of masses of the image in the far field and phase decomposition in the near field by Zernike polynomials [36,37]. Fig 7 shows values of *Gradient*- and *Zernike*-tilt (G- and Z-tilt) of the wavefront of star 1 along x- and y- axis and their difference for 100 random realizations of atmosphere turbulence. Coordinates of G-tilt — angular coordinates (G_x, G_y) of center of masses of the star image, coordinates of Z-tilt (Z_x, Z_y) — angular coordinates of two tilts when the wavefront of radiation is decomposed on the basis of Zernike polynomials. You can see that the values of tilts of two types are close to each other, and the amplitude of their difference, accordingly, is substantially lower than the tilt amplitude. In the calculations it was obtained that RMS (root-mean-square deviation) of full (along x- and y- axes) G-tilt is 1.08 times less than RMS of Z-tilt — 0.4 arcsec vs 0.43 arcsec (for Kolmogorov model of turbulence with infinite L_0 the difference in values RMS is 1.07 times [38]).

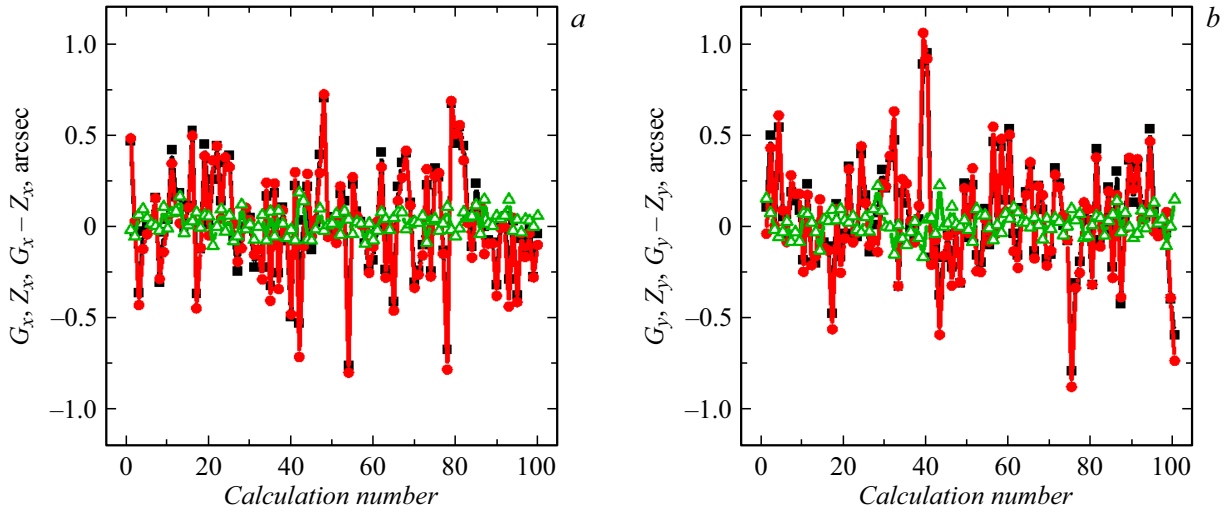

Figure 7. Coordinates of G-tilt (squares) and Z-tilt (circles) of wavefront of radiation from star 1 and their difference (triangles).

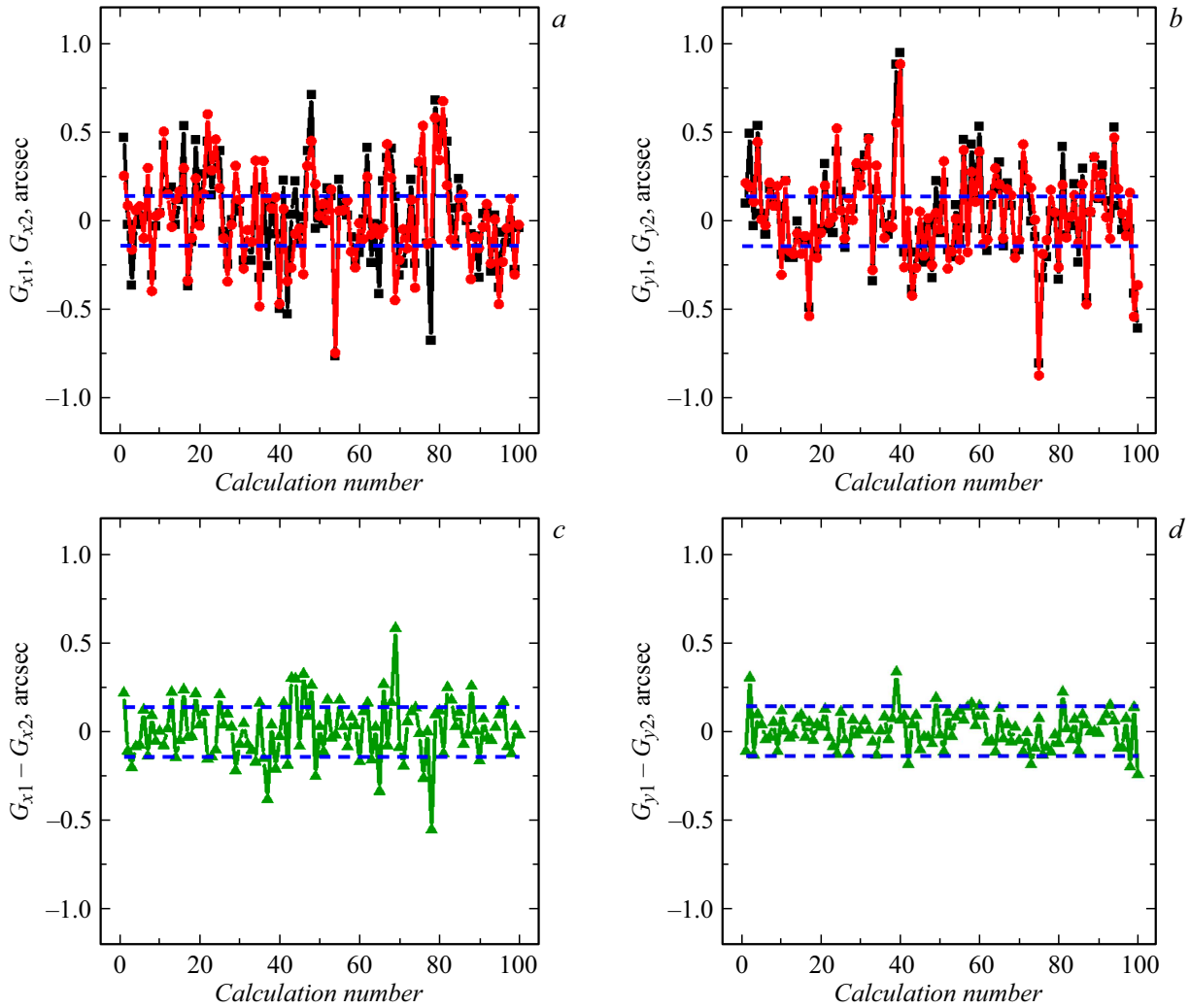

Figure 8. Coordinates of G-tilts (a, b) of star 1 (squares) and star 2 (circles) and their difference (c, d) for 100 random ralizations of turbulent atmosphere.

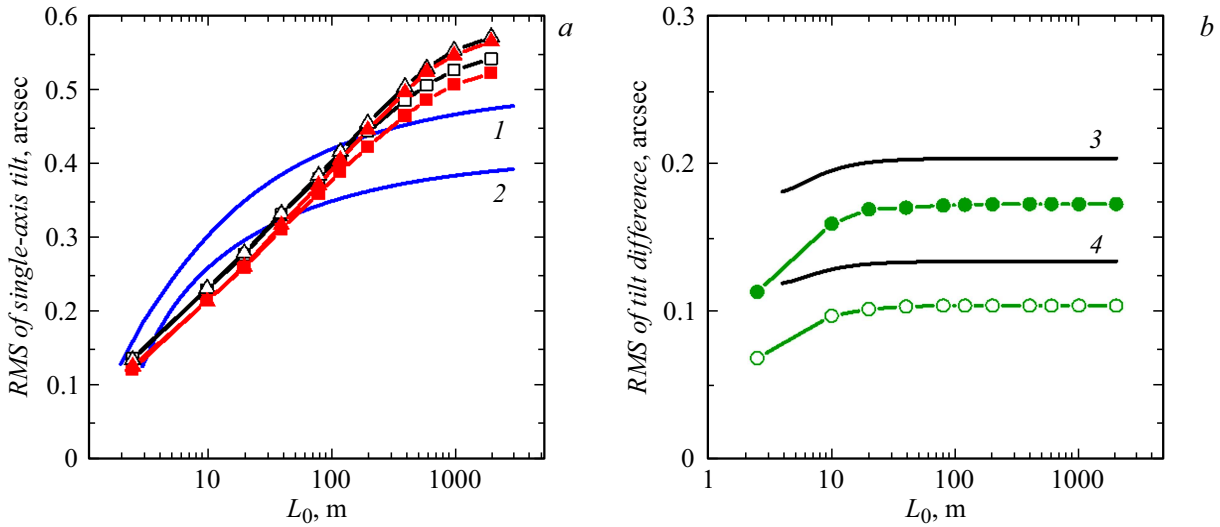

Figure 9. *RMS* of *G*-tilts of wavefront of star 1 and 2 along *x*- and *y*-axes (*a*) and *RMS* of *G*-tilts difference along *x*- and *y*-axes (*b*) in the calculations (curves with markers) and from analytical estimates (curves without markers) at different values of the outer turbulence scale L_0. Open markers: squares — σ_{x1}, triangles — σ_{y1}, circles — $\sigma_{\Delta y}$. Solid markers: squares — σ_{x2}, triangles — σ_{y2}, circles — $\sigma_{\Delta x}$. *1* — σ_S, *2* — σ_L, *3* — $\sigma_{\Delta x}$, *4* — $\sigma_{\Delta y}$.

Angular coordinates of *G*-tilt of wavefront from two stars for 100 random realizations of atmosphere turbulence are shown in Fig. 8, *a, b*. Hereinafter indices 1 and 2 indicate ratio of the parameter to star 1 and 2, accordingly. A dash indicates a level corresponding to the diffraction half-angle $0.5\theta_{\text{dif}} = 0.14$ arcsec. Quite high correlation of wavefront tilts is seen from two stars both in direction x, and by y. In general the amplitude of tilt fluctuations does not exceed $2\theta_{\text{dif}}$. From Fig. 8, *c, d* you can see that the amplitude of tilt difference fluctuations does not exceed θ_{dif} in direction of x and $0.5\theta_{\text{dif}}$ by y, which serves as an approximate level of angular error in definition of the coordinate of star 2.

Fig. 9, *a* shows *RMS* of tilts of wavefront σ_{x1}, σ_{x2} and σ_{y1}, σ_{y2} along *x*- and *y*-axes for two stars depending on L_0. Calculated dependences $\sigma_{x1}(L_0)$, $\sigma_{y1}(L_0)$, $\sigma_{x2}(L_0)$, $\sigma_{y2}(L_0)$ grow monotonously with growth of L_0 and, besides, $\sigma_{x1} \approx \sigma_{y1}$, $\sigma_{x2} \approx \sigma_{y2}$ with accuracy of not worse than 5% at specified L_0, which is compliant with the ideas of turbulence isotropism.

Fig. 9, *a* also shows approximated analytical dependences [38,39]. In [38] there is an analytical expression given to assess *RMS* of tilt of wavefront at $\eta = D/L_0 \ll 1$:

$$T = T_S \approx \left[\frac{6.08\mu_0}{D^{1/3}}\left(1 - 1.42\eta^{1/3} + 3.70\eta^2 - 4.01\eta^{7/3} + 4.21\eta^4 - 4.00\eta^{13/3}\right)\right]^{1/2}, \tag{10}$$

where

$$\mu_0 = \int_0^\infty C_n^2(\xi)d\xi,$$

integration is carried out along a vertical path. Expression (10) is derived in neglecting the diffraction and under the condition that $l_0 = 0$, and L_0 does not depend on z.

In [39] another formula is proposed to assess *RMS* of angular deviation of star image in the focal plane of the telescope:

$$T = T_L \approx \left[3.23R^{-1/3}r_0^{-5/3}k^{-2}\left(1 - 2^{-1/6}(\kappa_0^* R)^{1/3}\right)\right]^{1/2},$$

$$r_0 \approx \left(k^2 \int_0^\infty C_n^2(\xi)d\xi\right)^{-3/5},$$

$$(\kappa_0^*)^{-1} = \left(\int_0^\infty C_n^2(\xi)\kappa_0^{1/3}d\xi \Big/ \int_0^\infty C_n^2(\xi)d\xi\right)^{-3}, \tag{11}$$

where R — effective radius of Gaussian aperture, $\kappa_0^* = 2\pi/L_0^*$, L_0^* — effective outer scale of turbulence. Expression (11) is derived under the condition $(\kappa_0^* R)^{-1} \gg 1$ for the exponential model of spectral density of the refraction index [39], which is somewhat different from the widely available von Karman spectrum:

$$\Phi_n(\kappa_\perp, \kappa_z) = 0.033C_n^2(\kappa_\perp^2 + \kappa_z^2)^{-11/6}\left[1 - \exp\left(\frac{\kappa_\perp^2 + \kappa_z^2}{\kappa_0^2}\right)\right].$$

In our case $L_0^* = L_0$, $R = 50$ cm. Owing to isotropism of turbulence, *RMS* of wavefront tilt along two mutually perpendicular directions is $\sigma_S = T_S/\sqrt{2}$ and $\sigma_L = T_L/\sqrt{2}$.

Taking into account the fact that formulae (10) and (11) were derived with some simplifying assumptions, you may report the qualitative agreement of calculated and analytical dependences. You can see that with growth of L_0, as in the

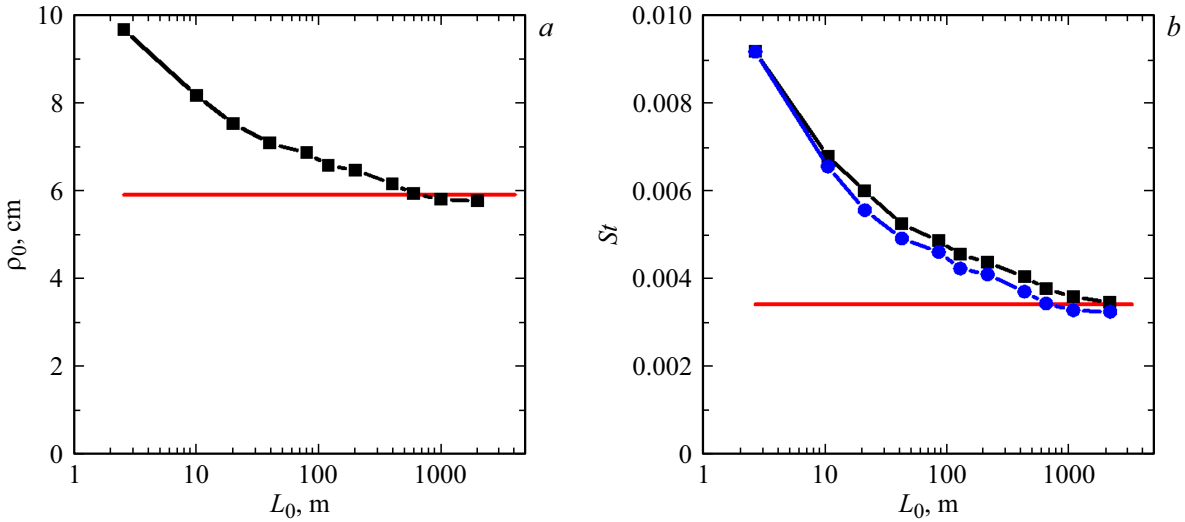

Figure 10. Radius of atmosphere coherence (a) and Strehl number of radiation from the star under long-term exposure (b) at different values L_0. Squares — calculated values, circles — analytical estimate, horizontal line — limit analytical value at $L_0 = \infty$.

Kolmogorov turbulence theory, the estimated dependences reach the plateau.

Fig. 9, b presents dependences of *RMS* of G-tilts difference for two stars on L_0. Analytical expression to assess *RMS* difference of tilts along x- and y-axes — $\sigma_{\Delta x}$ and $\sigma_{\Delta y}$ may be presented as follows [4]:

$$\begin{bmatrix}\sigma_{\Delta x}\\ \sigma_{\Delta y}\end{bmatrix} = \begin{bmatrix}\sigma_{\Delta x0}\\ \sigma_{\Delta y0}\end{bmatrix} (1 - 20.6\eta^2 + 27.4\eta^{7/3} + \ldots)^{1/2}, \quad (12)$$

where $\sigma_{\Delta x0}$ and $\sigma_{\Delta y0}$ — corresponding values at $L_0 = \infty$. Mathematical expressions for $\sigma_{\Delta x0}$ and $\sigma_{\Delta y0}$ have a rather bulky appearance and are not provided here, you may find them in [4]. Their assessment yields $\sigma_{\Delta x0} \approx 0.2$ arcsec and $\sigma_{\Delta y0} \approx 0.13$ arcsec. Dependences $\sigma_{\Delta x}(L_0)$ and $\sigma_{\Delta y}(L_0)$ grow monotonously to $L_0 = 10$ m and do not change further (at the same time dependences $\sigma_{x1}(L_0)$, $\sigma_{y1}(L_0)$ in Fig. 9, a continue growing monotonously approximately to $L_0 = 2000$ m). The progress of estimated curves in Fig. 9, b is qualitatively compliant with the analytical dependence (12). At $L_0 > 10$ m *RMS* the differences of wavefront tilts are 1.8 times higher along the axis of angular separation of stars x, vs along the perpendicular direction y, which is compliant with theoretical ideas [38]. Our calculated values are lower than the assessed ones approximately by 20–30%. *RMS* of differential tilt $\sigma_\Delta = \sqrt{\sigma_{\Delta x}^2 + \sigma_{\Delta y}^2}$ is approximately equal to 0.2 arcsec, which is 1.4 times lower than the full angle of diffraction divergence on the aperture. Parameter σ_Δ — that is the *RMS* of tilts of wavefront from star 2 after their adaptive phase correction using tilts from star 1.

Fig. 10, a shows calculated dependence of coherence radius of the vertical atmospheric path on the value of the outer scale of turbulence. The calculations used formula $\rho_0 = 0.98\lambda/\theta_{FWHM}$.

You can see that as L_0 grows, dependence $\rho_0(L_0)$ tends to the value of Fried parameter r_0, calculated using formula (1) with account of dependence $C_n^2(z)$ (horizontal line in Fig. 10, a). Fig. 10, b shows calculated and assessed dependence of Strehl number *St* [40] of star radiation. Under long-term exposure $St \approx \left(1 + (D/\rho_0)^2\right)^{-1}$ [41]. Data to build analytical dependence are taken from Fig. 10, a. The limit value of parameter *St* (horizontal line in Fig. 10, b) is calculated at $\rho_0 = r_0$.

Conclusion

In the paper, within the quasi-optical computational model, calculations were completed on radiation propagation from two natural stars via turbulent atmosphere to the telescope located on the Earth, with account of finiteness of the external turbulence scale L_0. The ratio of diameter of the telescope receiving aperture D to Fried parameter — around 17, which indicates difficult conditions for astronomic observations, if they are carried out without adaptive optics. The angular distance between stars is equal to 10 arcsec, which substantially exceeds the isoplanatic angle with account of all optical aberrations of the path (0.6 arcsec), and aberrations only for the „tilt“ (2.13 arcsec). Verification of the computational model was carried out by comparison of calculated and analytical structural functions of the radiation phase.

The calculations analyzed amplitude-phase characteristics of radiation from two stars in the near and far field, and modelled phase correction of radiation with account of anisoplanatism. It was demonstrated that use of radiation of star 1 as a reference for correction of phase distortions in radiation of star 2 and building of its image is not effective, which indicates the need of „ignition“ of LGS in direction of star 2 for correction of higher optical aberrations. In this case, taking into account the uncertainty of tilt of LGS radiation wavefront, you may use information in the tilt of star 1 radiation wavefront (by center of masses of the image

or from decomposition by Zernike polynomials). Then you can obtain an image of star 2 of practically diffraction quality, but its angular coordinate is displaced for difference of tilts from stars 1 and 2. The calculated dependence RMS is found for each of tilts and their difference from the outer turbulence scale L_0. Value RMS of tilts and their difference monotonously increases as L_0 increases and reaches the plateau at $L_0 \gg D$, as predicted by the theory. Calculated values RMS of tilt difference are lower than analytical estimates by 20−30%. It is interesting that the dependence RMS of tilt difference on L_0 reaches the plateau much earlier that the similar dependence for each individual tilt. In calculations of RMS of tilt difference is approximately equal to 0.2 arcsec at $L_0 > 20$ m, which is 1.4 times lower than the full angle of diffraction divergence.

To conclude, note that the developed computational model that was approved and confirms the results of approximated analytical models, may be used to determine the qualitative impact of anisoplanatism during astronomic observations using LGS technique and adaptive optics at different angular distance between the studied object and different reference sources in the wide range of turbulence conditions, including its non-Kolmogorov features.

Funding

This study was conducted within the scientific program of the National Center for Physics and Mathematics, section No. 4. Stage 2023-2025.

Conflict of interest

The authors declare that they have no conflict of interest.

References

[1] L.C. Andrews, R.L. Phillips. *Laser Beam Propagation Through Random Media* (SPIE Press, Bellingham, 2005)
[2] S.S. Veniaminov. *Kosmichesky musor. Tekhnogennoe zasorenie kosmosa i ego posledstviya* (IKI RAN, M., 2023), p. 204 (in Russian). DOI: 10.21046/spacedebris-2023
[3] R.K. Tyson. *Principles of Adaptive Optics* (Academic Press, Boston, 1991)
[4] J.W. Hardy. *Adaptive Optics for Astronomical Telescopes* (Oxford University Press, NY., 1998)
[5] F. Roddier. *Adaptive Optics in Astronomy* (Cambridge University Press, UK., 1999)
[6] V.P. Lukin. *Atmosfernaya adaptivnaya optika* (Nauka, Novosibirsk, 1986) (in Russian)
[7] R.Q. Fugate. Opt. Photon. News, **4** (6), 14 (1993). DOI: 10.1364/OPN.4.6.000014
[8] R. Foy. In: *Optics in Astrophysics,* ed. by R. Foy, F.C. Foy (Springer, Dordrecht, 2006), p. 249. DOI: 10.1007/1-4020-3437-7_15
[9] R. Foy, A. Migus, F. Biraben, G. Grynberg, P. McCullough, M. Tallon. Astron. Astrophys. Suppl. Ser., **111** (June II), 569 (1995).
[10] V.P. Lukin, B.V. Fortes. Atmos. Oceanic Opt., **10** (1), 34 (1997).
[11] M.S. Belen'kii. Appl. Optics, **39** (33), 6097 (2000). DOI: 10.1364/AO.39.006097
[12] L.A. Bolbasova, V.P. Lukin. Atmos. Ocean. Opt., **35** (S1), S165 (2022). DOI: 10.1134/s1024856023010037
[13] F.Yu. Kanev, V.P. Lukin. *Adaptivnaya optika. Chislennye i eksperimentalnye issledovaniya* (Izd-vo Instituta optiki atmosfery SO RAN, Tomsk, 2005)
[14] L.A. Bolbasova, V.P. Lukin. *Adaptivnaya korrektsiya atmosfernykh iskazheniy opticheskikh izobrazheniy na osnove iskusstvennogo opornogo istochnika* (Fizmatlit, M., 2012) (in Russian)
[15] H. Hemmati (ed.). *Near-Earth Laser Communications,* 2nd ed. (CRC Press, 2020). DOI: 10.1201/9780429186721
[16] J. Osborn, M.J. Townson, O.J.D. Farley, A. Reeves, R.M. Calvo. Opt. Express, **29** (4), 6113 (2021). DOI: 10.1364/OE.413013
[17] N. Martinez. Photonics, **10** (7), 858 (2023). DOI: 10.3390/photonics10070858
[18] D. Alaluf, J.M. Perdigues Armengol. CEAS Space J., **14**, 227 (2022). DOI: 10.1007/s12567-021-00392-2
[19] M. Cockram, N.M. Rey, A. Gilling, D. Alaluf. Proc. SPIE, **12777**, 127774E-1 (2023). DOI: 10.1117/12.2690830
[20] J.R. Beck, J.P. Bos. Proc. SPIE, **11506**, 115060N-1 (2020). DOI: 10.1117/12.2568975
[21] C.J. Pugh, J.-F. Lavigne, J.-P. Bourgoin, B.L. Higgins, T. Jennewein. Adv. Opt. Technol., **9** (5), 263 (2020). DOI: 10.1515/aot-2020-0017
[22] A.S. Gurvich, A.I. Kon, V.L. Mironov, S.S. Khmelevtsov. *Lazernoe izluchenie v turbulentnoy atmosfere* (Nauka, M., 1976) (in Russian)
[23] S.M. Rytov, Yu.A. Kravtsov, V.I. Tatarsky. *Vvedenie v statisticheskuyu radiofiziku. Ch. II. Sluchajnye polya* (Nauka, M., 1978) (in Russian).
[24] V.K. Ladagin. Voprosy atomnoy nauki i tekhniki. Ser. Metodiki i programmy chislennogo resheniya zadach matematicheskoy fiziki, **1**, 19 (1985) (in Russian).
[25] T. Karman. *Aerodynamics* (McGraw-Hill, NY., 1963)
[26] A.N. Kolmogorov. DAN SSSR, **30** (4), 299 (1941) (in Russian).
[27] A.M. Obukhov. DAN SSSR, **32** (1), 22 (1941) (in Russian).
[28] V.P. Kandidov, M.P. Tamarov, S.A. Shlyonov. Atmos. Oceanic Opt., **11** (1), 23 (1998).
[29] V.P. Kandidov, V.I. Ledenev. Radiophys. Quantum Electron., **24**, 301 (1981). DOI: 10.1007/BF01034765
[30] S.S. Chesnokov, V.P. Kandidov, S.A. Shlenov, M.P. Tamarov. Proc. SPIE, **3432**, 14 (1998). DOI: 10.1117/12.327984
[31] E.M. Johansson, D.T. Gavel. SPIE, **2200**, 372 (1994). DOI: 10.1117/12.177254
[32] R.N. Wilson. *Reflecting Telescope Optics II. Manufacture, Testing, Alignment, Modern Techniques* (Springer-Verlag, Berlin, Heidelberg, 1999)
[33] M. Esseling. *Photorefractive Optoelectronic Tweezers and Their Applications* (Springer International Publishing, Switzerland, 2015), DOI: 10.1007/978-3-319-09318-5
[34] A.V. Nemtseva, V.A. Bogachev, F.A. Starikov. Proc. SPIE, **12341**, 123411D-1 (2022). DOI: 10.1117/12.2644979
[35] A.V. Nemtseva, V.A. Bogachev, F.A. Starikov. Proc. SPIE, **12780**, 127801F-1 (2023). DOI: 10.1117/12.2690981
[36] F. Zernike. Mon. Not. R. Astron. Soc., **94**, 377 (1934).
[37] R.J. Noll. J. Opt. Soc. Amer., **66** (3), 207 (1976). DOI: 10.1364/JOSA.66.000207

[38] R.J. Sasiela. *Electromagnetic Wave Propagation in Turbulence: Evaluation and Application of Mellin Transforms* (Springer-Verlag, Berlin, Heidelberg, 1994), DOI: 10.1007/978-3-642-85070-7
[39] V.P. Lukin, V.V. Nosov, A.V. Torgaev. Appl. Optics, **53** (10), B196 (2014). DOI: 10.1364/AO.53.00B196
[40] K. Strehl. Z. Instrumentenkd, **22** (July), 213 (1902).
[41] H.T. Yura. J. Opt. Soc. Am., **63** (5), 567 (1973).

Translated by M.Verenikina